ASTRONOMY & ASTROPHYSICS
SUPPLEMENT SERIES

Astron. Astrophys. Suppl. Ser. **129,** 31-40 (1998)

Galaxy redshifts in 3 medium–distant clusters⋆

A. Cappi[1], **E.V. Held**[2,1], **and B. Marano**[1]
[1] Osservatorio Astronomico di Bologna, I–40126 Bologna, Italy
e–mail: cappi@astbo3.bo.astro.it, marano@astbo3.bo.astro.it
[2] Osservatorio Astronomico di Padova, Vicolo dell'Osservatorio, I-35122 Padova, Italy
e–mail: held@astrpd.pd.astro.it

Received August 1; accepted September 15, 1997

Abstract. We present results from spectroscopic observations of 3 rich and moderately distant galaxy clusters at the 3.6 m ESO telescope at La Silla. We measured 54 galaxy redshifts in 3 fields centered on the clusters A 3663 and A 3889, which are rich ($R = 2$) and distant ($D = 6$) ACO clusters, and on a new cluster, Cl 0053−37, identified on a deep plate. We present estimates of their velocity dispersion and virial mass. Cl 0053−37 had been noted as a concentration in a poor ACO cluster, S0102, with distance class $D = 4$. We show that Cl 0053−37 is a more distant cluster, connected to a large scale–structure at $z \sim 0.165$.

Key words: galaxies: clusters of — distances and redshifts — cosmology: observations — galaxies: clusters: Cl 0053−37; A 3663; A 3889

1. Introduction

The detection of clusters at medium and high redshift is a very efficient way to study a large number of distant galaxies with a reasonable amount of observing time, and to have fairly representative "normal" galaxies.

It has become apparent that galaxies in clusters have probably undergone a significant evolution in the last billion years, and a lot of work has been done after the discovery by Butcher & Oemler (1978, 1984) of evolutionary phenomena in clusters at $z \sim 0.4$. At the same time, given the observational evidence of an increasing excess in counts of galaxies, attributed to a population of faint blue galaxies (see Koo & Kron 1992; Ellis 1997, and references therein), the difference in the evolution of field and cluster galaxies, with the distinction of the roles played by the initial conditions and the environment (the "nature or nurture" dilemma), have yet to be clarified.

An estimate of the velocity dispersion, which measures the potential of the cluster and is therefore related to the cluster X–ray temperature (see Edge & Stewart 1991), allows an estimate of the virial mass and gives valuable information on cluster dynamics and the degree of subclustering (Malumuth et al. 1992; Hill & Oegerle 1993, and references therein), and can constrain models of galaxy formation (Evrard 1989; Peebles et al. 1989; Frenk et al. 1990). The cluster velocity dispersion is also correlated with other cluster parameters such as richness or luminosity, and has recently been used to define a Fundamental Plane of galaxy clusters (Schaeffer et al. 1993).

Moreover, cluster redshift measurements provide essential information for the study of large–scale structure using clusters. Present studies are limited at about $z = 0.1$ (~ 300 h^{-1} Mpc, where $h = H_0/100$; e.g. Cappi & Maurogordato 1992), but in the future it should be possible to have cluster redshift surveys deep and large enough to test much larger scales, where homogeneity should be achieved.

Motivated by the above discussed considerations, we began an observational program aimed at studying the photometric and spectral properties of medium–distant clusters. Galaxy clusters at intermediate redshifts ($z \sim 0.2$) can be found in the Abell (1958) and ACO (1989) catalogs. For the identification of more distant cluster candidates, we inspected deep prime focus plates taken at the 3.6 m ESO telescope by one of us for other purposes (Marano et al. 1988). These plates have a relatively large field (about 0.8 square degrees) and a relatively deep limiting magnitude ($J \sim 23.5$). Simulations tell us that at this magnitude limit we can hope to detect clusters at $z = 0.4$, and the richest ones at $z = 0.6$, assuming no evolution (Cappi et al. 1989).

Distant clusters are efficiently observed using multislit systems, which cover a small field and provide precise sky subtraction. Redshifts of at least ~ 20 cluster members are needed to have a significant estimate of the cluster velocity dispersion. The ESO Faint Object Spectrograph and Camera (EFOSC; Melnick et al. 1989) at the 3.6 m

Send offprint requests to: A. Cappi

⋆ Based on observations collected at the European Southern Observatory, La Silla, Chile.

Table 1. Data on selected clusters

Cluster name	$l_{\rm II}$	$b_{\rm II}$	Type	$N_{\rm A}$	R	D	m_3	m_{10}
A 3663	345.94	−32.54	R III	84	2	6	19.0	19.3
A 3889	18.16	−60.00	R II	95	2	6	18.6	19.4
Cl 0053−37	297.94	−79.54	IR	—	—	—	—	
S0102	298.15	−79.68	IR II	29	0	4	15.0	16.3

Table 2. Heliocentric redshifts of galaxies in Cl 0053−37

No.	RA (J2000)	DEC (J2000)	V	σ_V	Redshift	Note
1	00:56:10.23	−37:34:07.9	51570	282	0.17202	
2	00:56:09.22	−37:33:59.5	50799	51	0.16945	
3	00:56:07.07	−37:33:49.4	51628	138	0.17221	
4	00:56:09.71	−37:33:39.9	50709	120	0.16915	
5	00:56:01.49	−37:33:31.6	49315	111	0.16450	
6	00:56:06.41	−37:33:18.0	49754	154	0.16596	
7	00:55:57.50	−37:32:51.5	46839	38	0.15624	
8	00:55:58.90	−37:33:00.7	48490	50	0.16175	
9	00:56:02.76	−37:33:03.9	49588	192	0.16541	
10	00:56:04.76	−37:33:00.3	50394	117	0.16810	
11	00:56:04.75	−37:32:51.0	51594	84	0.17210	
12	00:55:55.59	−37:32:20.2	48514	145	0.16183	
13	00:55:56.74	−37:32:35.4	49555	123	0.16530	
14	00:55:57.74	−37:32:23.4	48256	101	0.16096	
15	00:55:59.32	−37:32:35.2	49041	145	0.16358	
16	00:55:59.09	−37:32:18.2	48888	117	0.16307	
17	00:56:01.32	−37:32:41.9	50168	187	0.16734	
18	00:56:02.45	−37:32:18.0	47381	138	0.15805	
19	00:56:02.41	−37:32:05.7	49097	113	0.16377	
20	00:55:56.18	−37:31:48.3	49439	14	0.16491	
21	00:56:09.54	−37:31:49.0	49863	107	0.16633	
B	00:55:55.48	−37:33:07.8	81639	20	0.27232	[OII] 3727 Å

telescope, having both imaging and multi–object spectroscopic capability, was well suited for our program.

In Sect. 2 the main characteristics of our three clusters are described; Sect. 3 presents the observations and the procedures followed for data reduction; Sect. 4 shows the results, which include the measure of cluster redshifts and velocity dispersions (virial masses were also determined for A 3889 and Cl 0053−37). In Sect. 5 we discuss the environment of cluster Cl 0053−37, showing that it is probably in a supercluster at $z \sim 0.165$.

2. The clusters

In this paper we present spectroscopic data on three clusters at moderate distances. The first two, A 3663 and A 3889, with richness class $R = 2$ and distance class $D = 6$ and no previously measured redshifts, were selected from the ACO catalog (Abell et al. 1989), the southern extension of the original Abell catalog (Abell 1958).

Another candidate was selected by visual inspection on a deep plate taken at the prime focus of the ESO 3.6 m telescope. After a check with the DIRA2 and NED databases, we realized that our distant candidate Cl 0053−37 (named after its coordinates at 1950) was at about 8 arcmin south–east of the center of a poor ACO cluster, listed in the ACO Supplementary List of Clusters as S0102. The distance class of S0102 is $D = 4$, and the magnitude of its 10th member is 16.3, but a question mark in the table warns that the measure is not reliable. A note points to a "curious linear concentration S−E of center", i.e. to our candidate, which is indeed characterized by an elongated shape. On the basis of its appearance on the plate, we suspected that this concentration was indeed a background cluster.

The main data concerning the above three clusters are listed in Table 1, where name, galactic longitude and latitude $l_{\rm II}$ and $b_{\rm II}$, Abell type (Regular or IRregular), Bautz–Morgan type, Abell number $N_{\rm A}$, richness R, distance class D, and J magnitude of the 3rd and 10th brightest member are given for each cluster. We also report the characteristics of S0102. We selected the galaxies to be observed in

the central parts of the clusters, typically within 0.5 Abell radii ($R_A = 1.5\ h^{-1}$ Mpc).

3. Observations and data reduction

We observed the selected clusters with EFOSC at the Cassegrain focus of the ESO 3.6 m telescope at La Silla (30 Sept.– 2 Oct. 1989). We obtained images of the fields with EFOSC; then, we selected the objects and we prepared the masks for multi–object spectroscopy with PUMA (Soucail et al. 1987). Three masks were employed for A 3889, two masks for Cl 0053−37, and one for A 3663. Integration times were 3600 s. The finding charts of all galaxies with measured redshift are given in Figs. 1–3.

The spectroscopic observations were accomplished using EFOSC in MOS mode, with the B300 grism (which gives a dispersion of 230 Å/mm). The RCA SID 006 EX Hi-Res. CCD detector (ESO CCD #8) was used in binned mode (see also Dupin et al. 1987; Giraud 1988; Soucail et al. 1988, for details on the MOS technique). The B300 grism gives a resolution of 7 Å per pixel over a spectral range between 3600 and 7200 Å; the effective range depends however on the position of the galaxy on the CCD. Spectra were wavelength calibrated using a He–Ar lamp.

Data reduction was performed using the ESO package MIDAS. Spectra were reduced in the standard way, by bias subtraction and flat–fielding of the science frame. Central columns with high S/N ratio were coadded, cosmic rays removed, then the object spectra were wavelength calibrated using a He–Ar lamp and sky subtracted. Usually for each galaxy spectrum we had a sky spectrum taken in a nearby position on the mask; when this was not the case (because of geometrical constraints on the masks in order to avoid overlapping of spectra) we used a mean sky spectrum.

As discussed by Garilli et al. (1991), cross–correlation techniques are not so effective when spectra are obtained through holes with EFOSC in MOS mode. To assure homogeneity of results, for all spectra (obtained with holes or slits) lines were identified and their centers were determined semi–automatically using a series of MIDAS routines. The good S/N ratio of the spectra allowed us easy identification and precise measurements of the line centers. At least 4 lines were used for each spectrum; the Balmer lines (from H_η to H_β), the CaII H & K lines, the G-band, the magnesium blend B were the most common absorption features.

In Tables 2–4, for each galaxy we report in the first column a number which allows identification on the finding charts, in the second and third columns right ascension and declination (J2000) as measured on Digitized Sky Survey scans, in the fourth column the measured heliocentric velocity, in the sixth column its internal error (estimated as the standard deviation of the velocities of individual lines), and in the seventh column the redshift (in the transformation from redshift to velocity we used $c = 299792.5$ km s^{-1}).

To test the reliability of our data, we also used the cross-correlation task XCSAO in IRAF to measure radial velocities for a few randomly chosen galaxy spectra, adopting two spectra of K stars as templates. The results are consistent with the redshifts obtained by line identification. Furthermore, a comparison of the redshifts from two spectra of the same galaxy observed in two successive runs gives a difference of 20 km s^{-1}, well below the quoted errors.

4. Results

For a dynamical analysis of the velocity data in Tables 2–4, allowance must be made for the fact that, even when velocity information is available, there is a certain degree of ambiguity about cluster membership. Thus, velocity dispersions were calculated by rejecting galaxies with a too high velocity relative to the mean, using the 3-σ clipping procedure of Yahil & Vidal (1977). Then the method described by Danese et al. (1980) was applied, in order to determine the 68% confidence uncertainties for cluster redshifts and velocity dispersions. This method assumes a Gaussian velocity distribution.

For our two best-studied clusters, Cl 0053−37 and A 3889, we collected 21 and 24 cluster galaxy spectra respectively, with negligible contamination from stars and background or foreground galaxies. Our estimates of mean velocity, velocity dispersion and virial mass are therefore not affected by undersampling (see Girardi et al. 1993).

Table 5 summarizes the global dynamical information derived from our analysis. Column 1 gives the cluster name, Col. 2 gives the number of cluster members with measured redshifts, Col. 3 gives the weighted mean heliocentric velocity. The mean redshifts referred to the Local Group (Yahil et al. 1977), $< z_c >$, are listed in Col. 4, while Col. 5 gives the radial velocity dispersion σ_r. Estimates of the cluster total velocity dispersions σ_t and virial masses are given in Cols. 6 and 7, and discussed below.

Whenever the velocity distribution is not well-matched by a Gaussian, one of the robust techniques described by Beers et al. (1990) is preferable. To have a feeling of the influence of the Gaussian hypothesis on our results, for all clusters we calculated the median velocity, the biweight location estimator, equivalent to the mean velocity of the Gaussian distribution, and the biweight scale estimator, equivalent to the velocity dispersion (C_M, C_{BI}, S_{BI} respectively in the notation of Beers et al. 1990). Table 6 gives the values of some robust estimators, assuming the same weight for all redshift measures: median velocity V_{med} (Col. 2), biweight estimate V_{biw} (Col. 3), and biweight velocity dispersion σ_{biw} (Col. 4). Errors are estimated from the standard deviation of 100 bootstrap samples. There is a very good agreement between the standard and the

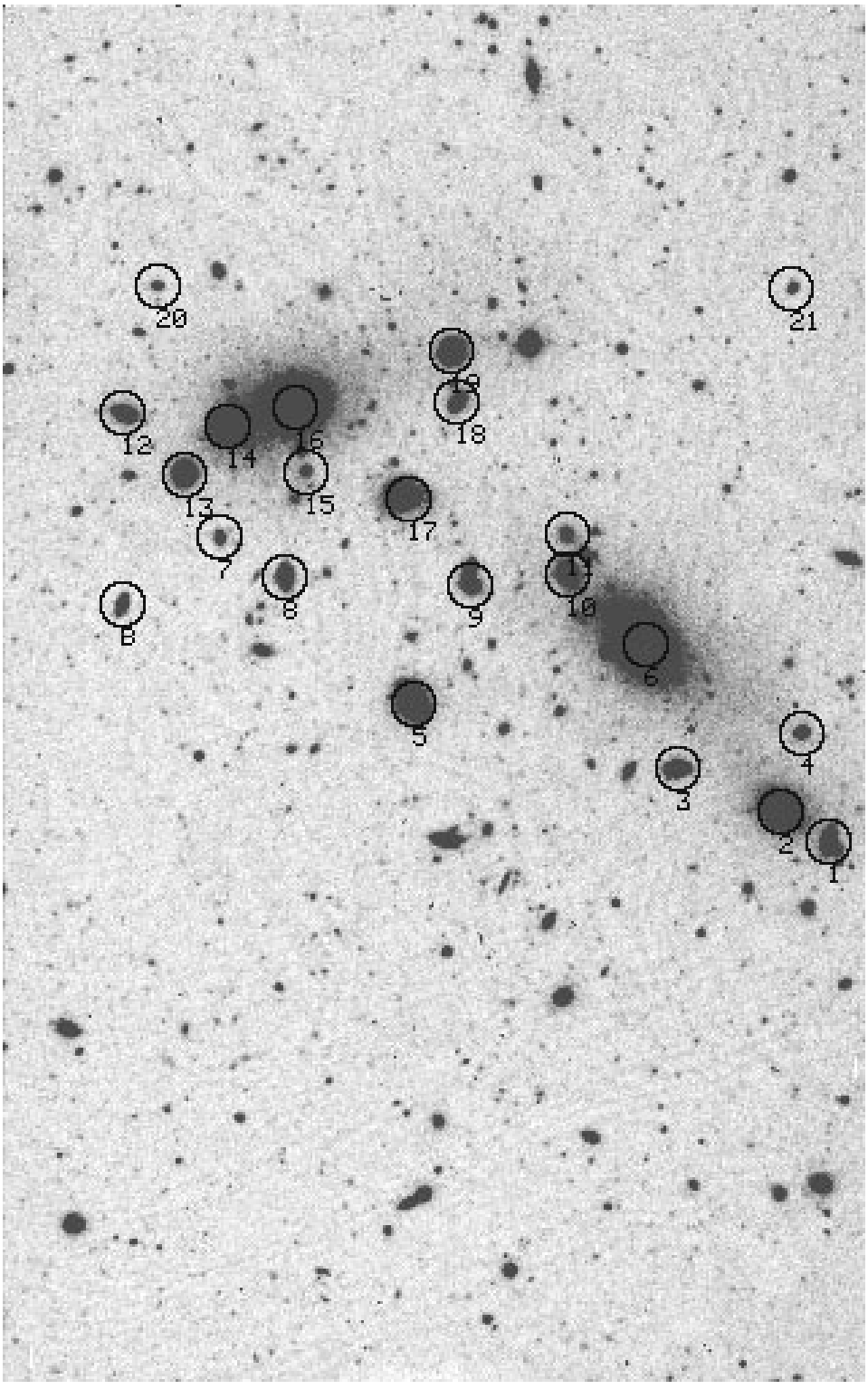

Fig. 1. Cl 0053−37: finding chart (in this as in the following finding charts, west is on the left and north is on the top). This cluster was considered part of the ACO poor cluster S0102; Abell et al. (1989) noticed it as a "curious linear concentration". B is a background galaxy at $z \sim 0.27$

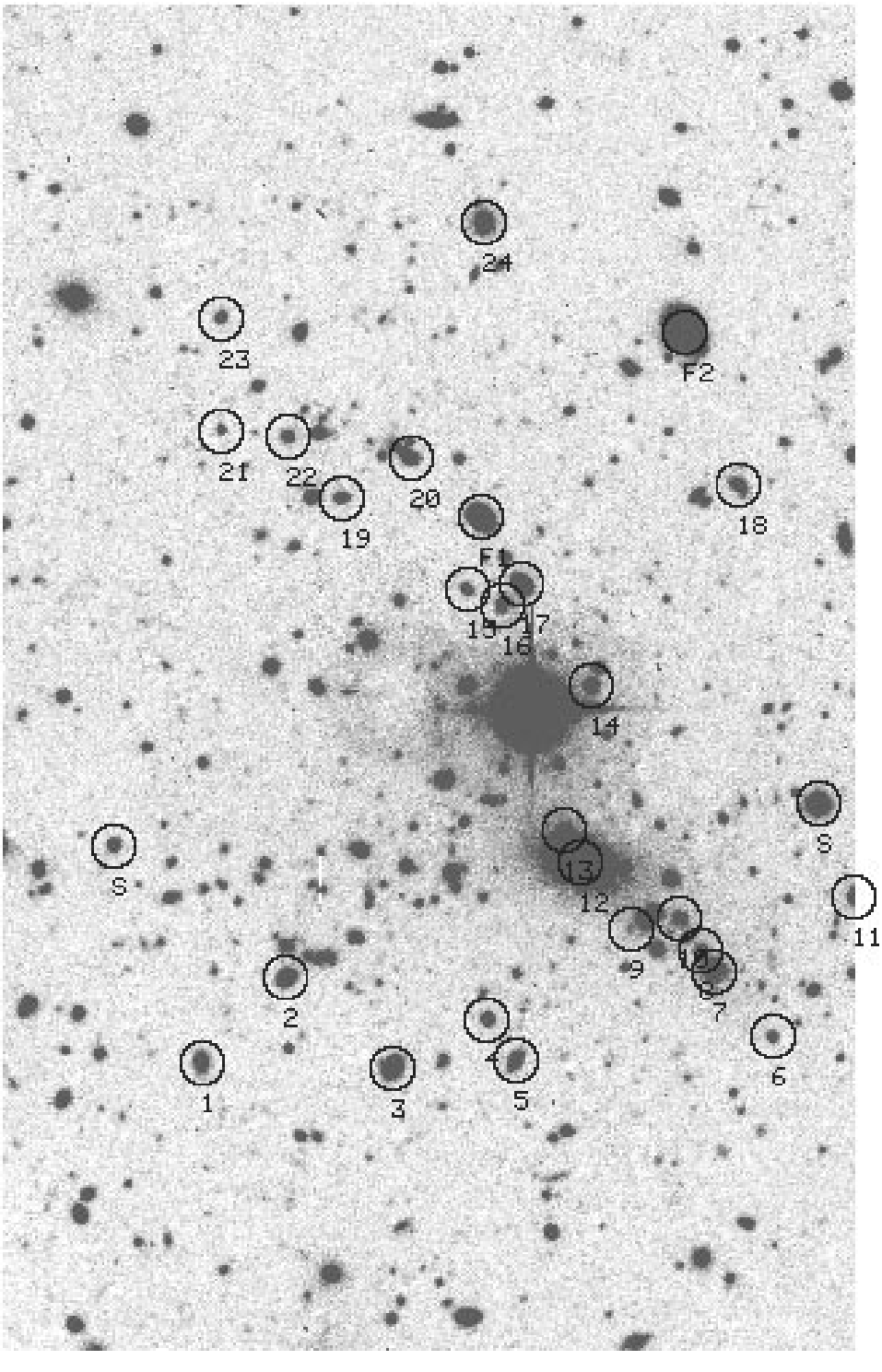

Fig. 2. A 3889: finding chart. F1 and F2 are two foreground galaxies at $z \sim 0.1$; S indicates a star

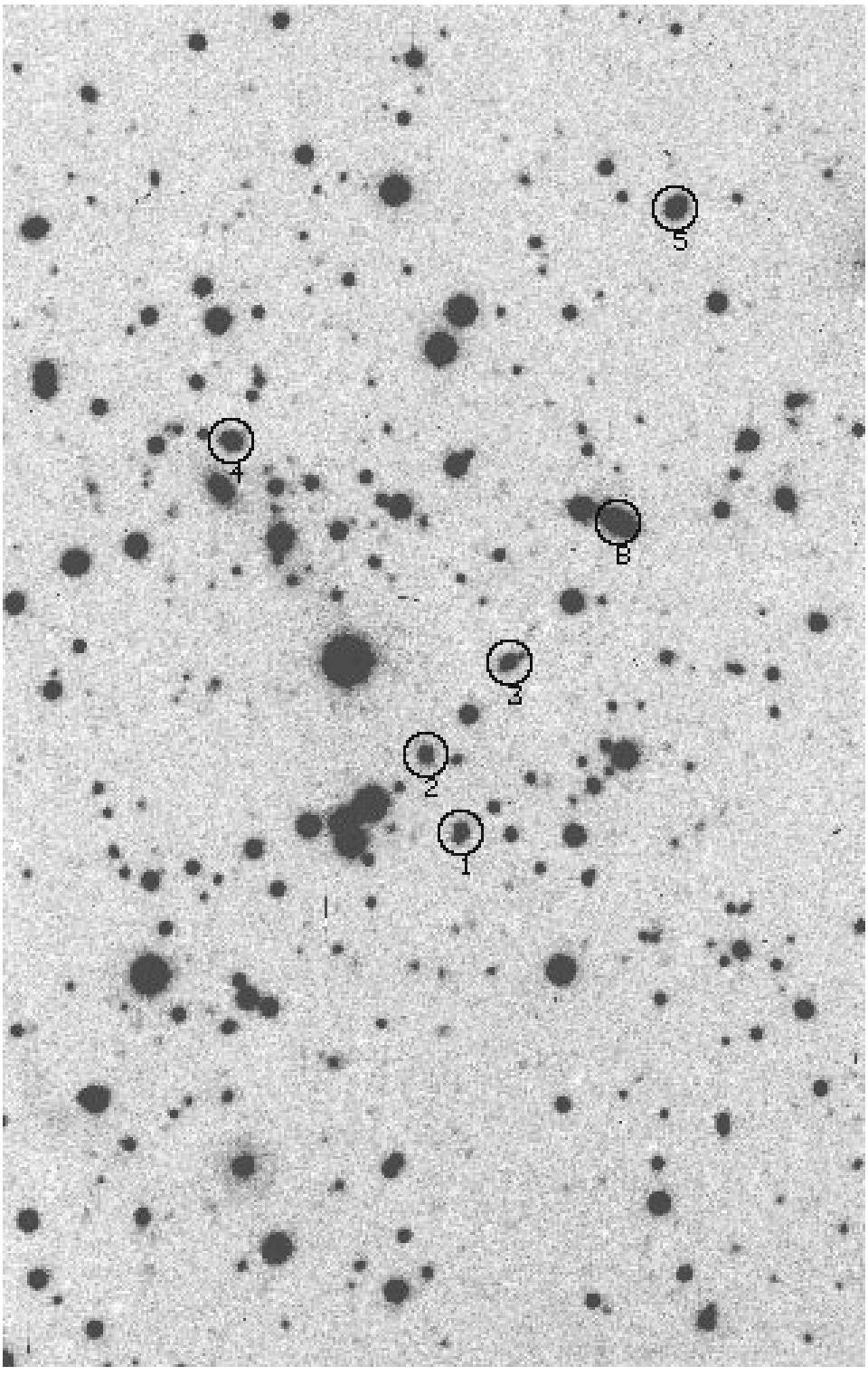

Fig. 3. A 3663: finding chart

Table 3. Heliocentric redshifts of galaxies in A 3889

No.	RA (J2000)	DEC (J2000)	V	σ_V	Redshift
1	22:34:44.68	−30:34:17.9	76661	176	0.25571
2	22:34:46.33	−30:33:57.5	73228	95	0.24426
3	22:34:48.37	−30:34:19.6	78120	108	0.26058
4	22:34:50.24	−30:34:07.7	74723	260	0.24935
5	22:34:50.80	−30:34:17.9	74479	304	0.24844
6	22:34:55.87	−30:34:13.7	76804	121	0.25619
7	22:34:54.62	−30:33:56.7	74623	85	0.24892
8	22:34:54.42	−30:33:51.0	76641	81	0.25565
9	22:34:53.34	−30:33:42.5	73741	111	0.24597
10	22:34:54.03	−30:33:42.3	76679	69	0.25577
11	22:34:57.43	−30:33:37.8	76210	118	0.25421
12	22:34:52.05	−30:33:28.7	74660	177	0.24904
13	22:34:51.79	−30:33:21.9	72590	107	0.24213
14	22:34:52.32	−30:32:44.5	76696	210	0.25583
15	22:34:49.97	−30:32:18.9	75003	161	0.25018
16	22:34:50.61	−30:32:24.0	75283	53	0.25112
17	22:34:51.01	−30:32:18.1	73928	150	0.24660
18	22:34:55.22	−30:31:53.5	74498	200	0.24850
19	22:34:47.59	−30:31:56.8	74962	139	0.25005
20	22:34:48.87	−30:31:46.2	76783	264	0.25612
21	22:34:45.22	−30:31:38.1	74932	151	0.24995
22	22:34:46.54	−30:31:39.8	73734	172	0.24595
23	22:34:45.77	−30:31:09.8	74692	300	0.24915
24	22:34:50.36	−30:30:47.1	76923	420	0.25659
F1	22:34:50.22	−30:32:01.9	33306	148	0.11110
F2	22:34:54.20	−30:31:16.1	32862	124	0.10962

Table 4. Heliocentric redshifts of galaxies in A 3663

No.	RA (J2000)	DEC (J2000)	V	σ_V	Redshift	Note
1	20:07:12.44	−52:36:09.5	69709	240	0.23252	[OIII] doublet
2	20:07:11.49	−52:35:50.1	74040	274	0.24700	
3	20:07:13.76	−52:35:27.5	72886	534	0.24312	
4	20:07:06.26	−52:34:31.0	73222	189	0.24424	
5	20:07:18.47	−52:33:33.9	70035	234	0.23361	[OII] 3727 Å
B	20:07:16.75	−52:34:52.3	100076	573	0.33382	[OII] 3727 Å

robust estimates for these two clusters; the difference between median, biweight and mean velocity is $\sim$300 km s^{-1} for Cl 0053−37 and $\sim$400 km s^{-1} for A 3889, while the standard and biweight estimates of the velocity dispersion agree within 100 km s^{-1}.

We now give a short description of our results for individual clusters. For Cl 0053−37, we measured the redshifts of 22 galaxies in the frame: only one turned out to be a background galaxy with the [OII] 3727 Å emission line, at a redshift of 0.27, the remaining 21 spectra passing the 3-σ clipping test. None of them shows emission lines.

The velocity histogram, shown in Fig. 4a, appears quite symmetric. The mean heliocentric velocity of this cluster is $v = 49265$ km s^{-1}, and the redshift relative to the Local Group is $< z_c >= 0.1625 \pm 0.001$. The radial velocity dispersion is $\sigma_r = 1144^{+234}_{-145}$, and the total velocity dispersion (for an isotropic velocity distribution) is $\sigma = 1982^{+450}_{-317}$ km s^{-1}. It is clear that Cl 0053−37 cannot be part of S0102, unless the distance of the latter was underestimated by Abell et al. (1989). We will discuss this issue in the following section.

For A 3889, 24 of the 26 observed galaxies turned out to be true members of the cluster, passing the 3-σ clipping test; the remaining two are foreground galaxies (presumably belonging to a group) at $z \sim 0.11$. The mean observed velocity of the cluster is 75354 km s^{-1}, and the redshift is $z = 0.2517 \pm 0.001$. The measured radial velocity dispersion is 1119^{+210}_{-134} km s^{-1}, while the total velocity dispersion is 1939^{+405}_{-292} km s^{-1}, consistent with values determined for nearby rich clusters. The brightest galaxy

Table 5. Dynamical data

Cluster	N	$< V >$	$< z_c >$	σ_r	σ_t	mass ($M_\odot$)
Cl 0053−37	21	49265	0.1625 ± 0.0010	1144^{+234}_{-145}	1982^{+450}_{-317}	$2\,10^{15}$
A 3889	24	75354	0.2517 ± 0.0010	1119^{+210}_{-134}	1939^{+405}_{-292}	$3\,10^{15}$
A 3663	5	71861	0.2397 ± 0.0030	—	—	—

(No. 12) has a velocity of -694 km s^{-1}relative to the cluster mean velocity, but its velocity relative to the *median* velocity of the cluster is -287 km s^{-1}. Indeed, the velocity histogram (Fig. 4b) shows two main peaks. Since no apparent segregation is found across the field, if the peaks correspond to two real subclusters, they are mainly along the line-of-sight. The foreground peak is centered at $\sim$ 74500−75000 km s^{-1}, and the background one at $\sim$ 76500−77000 km s^{-1}.

We estimated the masses of these two clusters using the virial theorem (see Bahcall & Tremaine 1981; Malumuth et al. 1992). Assuming isotropic orbits and spherical symmetry,

$$M_{\rm vir} = \frac{3\pi D \sum_{i=1}^{N} \alpha_i v_{r,i}^2}{2G \sum_{i<j} \sum_{j=1}^{N} (\alpha_i \alpha_j / \theta_{ij})} \quad (1)$$

where D is the angular diameter distance of the cluster, $v_{r,i}$ is the difference between the velocity of galaxy i and cluster (mean) velocity, θ_{ij} is the angular separation between galaxy i and galaxy j, N is the total number of galaxies and α_i is the statistical weight of galaxy i. Giving the same weight ($1/N$) to all galaxies, we obtain $M_{\rm vir} \sim 2\ 10^{15} M_\odot$ for Cl 0053−37, and $M_{\rm vir} \sim 3\ 10^{15} M_\odot$ for A 3889, quite typical of rich clusters, even if these values can only be considered as rough estimates of the real mass.

More limited velocity data are available for the third cluster. A 3663 was observed in not very good weather conditions, and we lost some spectra because of their low signal–to–noise ratio. The small number of measured velocities does not allow a precise determination of the cluster redshift, especially because the spread is quite large: this is apparent in the difference between the median and the mean radial velocity of the cluster, $\sim$ 1000 km s^{-1}, while the biweight estimate gives an intermediate value (cf. Table 6). The standard deviation of the 5 measured radial velocities, divided by $(1 + z_c)$, gives $\sigma = 1590$ km s^{-1}; the biweight estimator gives a velocity dispersion $\sigma_{\rm biw} = 1704$ km s^{-1}. These values may represent an overestimate of the true radial velocity dispersion, and are only indicative. It is possible that these galaxies belong to different groups or subclusters, and more redshifts are needed to provide an answer. We also note that 2 out of the 5 observed galaxies have emission lines.

Our new results offer the opportunity to test the precision of redshift estimates (obtained from a relation between cluster redshift and magnitude of the tenth brightest galaxy, or a combination of the magnitudes of the first, third, and tenth brightest galaxies, with a possible correction for the cluster richness) at high distances. Using the relation given by Scaramella et al. (1991; their Eq. (1)), we find estimated luminosity distances equal to 860 h^{-1} Mpc for A 3889 and 920 h^{-1} Mpc for A 3663, while the luminosity distances calculated from our measured redshifts are respectively 797 h^{-1} Mpc and 757 h^{-1} Mpc. There is a well–defined relation between estimated and measured distances in the Abell and ACO catalogs, and our results confirm that, for the ACO catalog, such a relation can give reasonable results even at $z \sim 0.25$.

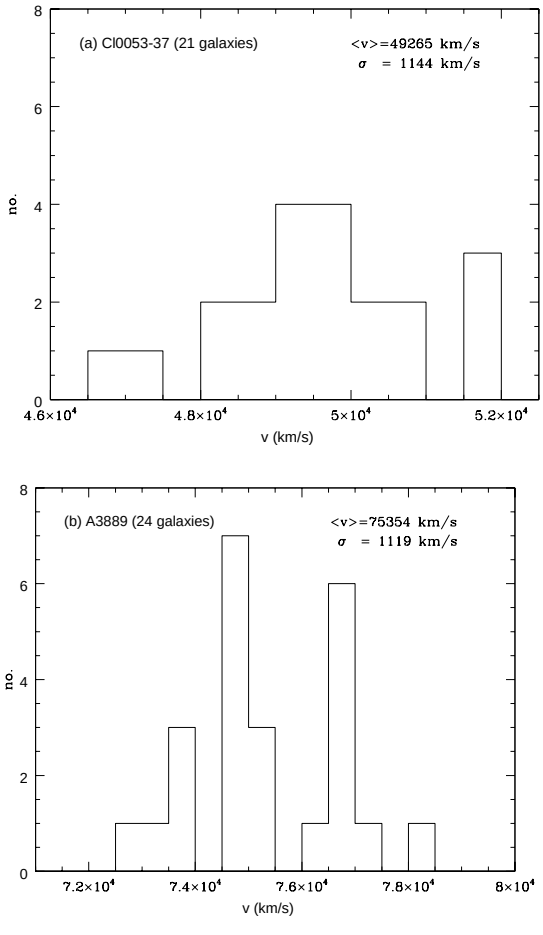

Fig. 4. a) Velocity histogram of cluster Cl 0053−37; **b)** velocity histogram of cluster A 3889

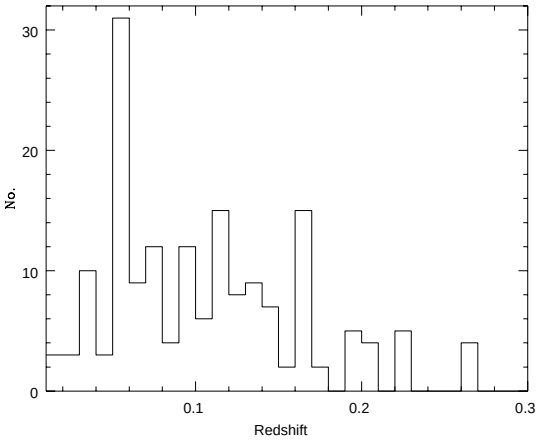

Fig. 5. Redshift histogram of the LCRS galaxies within 2 degrees of Cl 0053−37 center

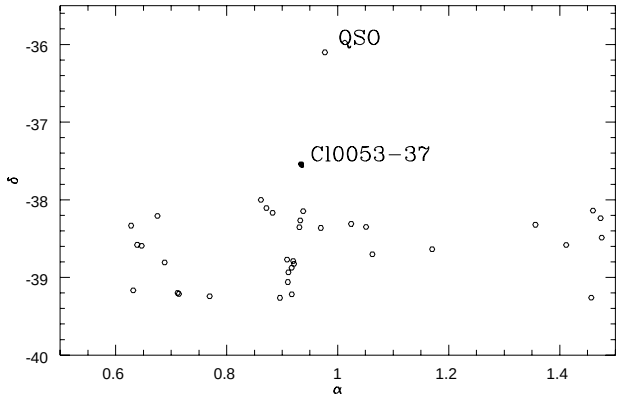

Fig. 6. Map of all LCRS galaxies with a redshift between 0.160 and 0.170, with Cl 0053−37 and a QSO

Table 6. Robust estimates of velocity and velocity dispersion

Cluster	$V_{\rm med}$	$V_{\rm biw}$	$\sigma_{\rm biw}$
Cl 0053−37	49555	49583 ± 261	1091 ± 215
A 3889	74947	75218 ± 452	1095 ± 220
A 3663	72886	72293 ± 1523	1704 ± 718

5. A supercluster at $z \sim 0.165$?

We will now discuss in some detail the nature and environment of the cluster Cl 0053−37. As we have already mentioned, Cl 0053−37 is visible in the field of the poor Abell cluster S0102. The first question, of course, is whether the former is a substructure of the latter.

For Cl 0053−37 we measured a redshift of $\sim$ 0.163, which is inconsistent with the estimated distance of S0102. Consequently there are two possibilities: either Cl 0053−37 is a true concentration in S0102 – in which case the distance class of S0102 would have been underestimated – or it is a background cluster seen through S0102. From visual inspection of the ESO field F295 which contains the cluster, the latter hypothesis seems more plausible. The redshift of a galaxy near the center of S0102 was measured by Bica et al. (1991), and is $z \sim 0.055$. More recently, S0102 was selected with an automatic algorithm in the EDCC survey (Collins et al. 1995) where it was identified as EDCC494: its redshift (on the basis of 3 galaxies) is $z \sim 0.056$. Therefore, it is clear that Cl 0053−37 is a new cluster, independent of S0102, seen in projection. However, it is unlikely that this background cluster could contaminate the estimate of the S0102 richness class, because the galaxies in Cl 0053−37 are significantly fainter than the members of S0102.

Now, it is interesting to note that there are two southern surveys not far from our cluster: the Las Campanas Redshift Survey (LCRS; Shectman et al. 1996) and the Eso Slice Project (ESP; Vettolani et al. 1997). In particular, the slice of the LCRS centered at $\delta = -39°$ (1.5 degrees wide) was checked to obtain other redshifts for Cl 0053−37 and to search for structures related to this cluster.

We used NED (which now includes LCRS) to look for all objects within 2 degrees from the cluster center. Nearly all of them belong to the first strip of the LCRS, and their redshift histogram is shown in Fig. 5. There are three main peaks: the first, at $z \sim 0.056$, corresponds to the redshift of S0102, the second one, at $z \sim 0.11$, probably corresponds to a large structure identified in the ESP some degrees below, the third, impressive peak (taking into account the decreasing selection function) is at $z \sim 0.165$, and corresponds to the redshift of Cl 0053−37.

Are these objects members of Cl 0053−37? Figure 6 shows the projected distribution of all galaxies in a redshift range $0.157 \leq z \leq 0.167$, corresponding to the peak in the histogram of Fig. 5. It is quite clear that we have a linear structure with a void quite well defined on the left, which crosses the whole 1.5 degrees of the LCRS strip, includes our cluster, and possibly also a QSO found at the same redshift (Hewitt & Burbidge 1989). If this QSO belongs to the same structure or not, is not possible to assess in the absence of other data.

At $z = 0.165$, 1 h^{-1} Mpc corresponds to about 9 arcmin ($q_0 = 0.5$): the objects in the LCRS reach distances more than 10 h^{-1} Mpc from the cluster center. This corresponds to a supercluster scale. All these elements suggest that Cl 0053−37 belongs to a larger, coherent structure with a possible size of 30 h^{-1} Mpc in the δ direction and along the line of sight. In the α direction it appears less extended, no more than a few Mpc h^{-1} Mpc, and it might be a wall between voids. The elongation of the cluster, originally remarked by Abell et al. (1989), does not follow the elongation of the large–scale structure defined by the LCRS galaxies, the quasar, and the cluster itself. Perhaps the cluster is at some intersection of structures; however, the exact topology of the region and a more detailed dynamical study will require further data.

6. Summary

We measured redshifts and velocity dispersion for two ACO clusters and a new cluster we identified on prime–focus plates, which had been previously included as part of the poor ACO cluster S0102 by Abell et al. (1989). As expected, they are medium–distant clusters, with redshifts between 0.16 and 0.25. For A 3889 and Cl 0053−37, we estimated also virial masses, finding respectively $M \sim 3\ 10^{15}\ M_{\odot}$ and $M \sim 2\ 10^{15}\ M_{\odot}$. We have presented strong evidence for a supercluster or wall at $z \sim 0.165$, to which Cl 0053−37 belongs.

This research has made use of: DIRA2, developed by the Astronet Working Group on Database and Documentation in Bologna, Italy; the NASA/IPAC Extragalactic Database (NED) which is operated by the Jet Propulsion Laboratory, California Institute of Technology, under contract with the National Aeronautics and Space Administration; the Digitized Sky Surveys (DSS), which were produced at the Space Telescope Science Institute under U.S. Government grant NAG W-2166. The images of these surveys are based on photographic data obtained using the Oschin Schmidt Telescope on Palomar Mountain and the UK Schmidt Telescope. The plates were processed into the present compressed digital form with the permission of these institutions.

References

Abell G.O., 1958, ApJ 3, 211
Abell G.O., Corwin, H.G., Olowin, R.P., 1989, ApJS 70, 1 (ACO)
Bahcall J.N., Tremaine S., 1981, ApJ 244, 805
Beers T.C., Flynn K., Gebhardt K., 1990, AJ 100, 32
Bica E., Pastoriza M.G., Da Silva L.A., Dottori H., Maia M., 1991, AJ 102, 1702
Butcher H., Oemler A., 1978, ApJ 219, 18
Butcher H., Oemler A., 1984, ApJ 285, 426
Cappi A., Chincarini G., Conconi P., Vettolani G., 1989, A&A 223, 1
Cappi A., Maurogordato S., 1992, A&A 259, 423
Collins C., Guzzo L., Nichol L.C., Lumsden S.L., 1995, MNRAS 274, 1071
Danese L., De Zotti G., di Tullio G., 1980, A&A 82, 322
Dupin J.P., et al., 1987, The Messenger 47, 55
Edge A.C., Stewart G.C., 1991, MNRAS 252, 428
Ellis R.S., 1997, ARA&A 35 (in press)
Evrard A.E., 1989, ApJ 341, L71
Fabricant D.G., McClintock E., Bautz M.W., 1991, ApJ 381, 33
Frenk, C.S., White S.D.M., Efstathiou G., Davis M., 1990, ApJ 351, 10
Garilli B., Maccagni D., Vettolani G., 1991, AJ 101, 795
Girardi M., Biviano A., Giuricin G., Mardirossian F., Mezzetti M., 1993, ApJ 404, 38
Giraud E., 1988, The Messenger 51, 37
Hewitt, A., Burbidge, G., 1989 ApJS 69, 1
Hill J.M., Oegerle W.R., 1993, AJ 106, 831
Koo D.C., Kron R.G., 1992, ARA&A 30, 613
Malumuth E.M., Kriss G.A., Van Dyke Dixon W., Ferguson H.C., Ritchie C., 1992, AJ 104, 495
Marano B., Zamorani G., Zitelli V., 1988, MNRAS 232, 111
Mellier Y., Soucail G., Fort B., Mathez G., 1988, A&A 199, 13
Melnick J., Dekker H., D'Odorico S., 1989, ESO Operating Manual No. 4
Peebles P.J.E., Daly R.A., Juskiewicz R., 1989, ApJ 347, 563
Scaramella R., Zamorani G., Vettolani G., Chincarini G., 1991, AJ 101, 342
Schaeffer R., Maurogordato S., Cappi A., Bernardeau F., 1993, MNRAS 263, L21
Schectman S.A., et al., 1996, ApJ 470, 172
Soucail G., Mellier Y., Fort B., Cailloux M., 1988, A&AS 73, 471
Soucail G., Mellier Y., Fort B., Picat J.P., Cailloux M., 1987, A&A 184, 361
Vettolani G., et al., 1997, A&A 325, 954
Yahil A., Tamman G.A., Sandage A., 1977, ApJ 217, 903
Yahil A., Vidal N.V., 1977, ApJ 214, 347